Research

Human Population Growth in Anthropocene: Active Soft Matter Perspective.

Drozd-Rzoska Aleksandra[1,*], Sojecka Agata Angelika[2,*]

1. Institute of High Pressure Physics of the Polish Academy of Sciences, Warsaw, Poland
2. Dept. Marketing, University of Economics in Katowice, Katowice, Poland

* Correspondence: Aleksandra Drozd-Rzoska: Ola.DrozdRzoska@gmail.com ; Agata Angelika Sojecka: agata.angelika.sojecka@gmail.com

Citation: Drozd-Rzoska A, Sojecka AA. Human Population Growth in Anthropocene: Active Soft Matter Perspective. Proceedings of Socratic Lectures. **2026**, 14, 2-25. https://doi.org/10.55295/PSL.14.2026.III1

Abstract:
Despite a long record of studies, the effective and fundamentally validated modelling of global population changes remains a challenge. One can recall puzzling forecasts up to 2100, and the significance of looking back, even to the onset of the Anthropocene. This report presents the recently developed Human Intelligent (HI) Active Soft Matter (ASM) concept as the fundamental reference. It is validated by describing the dynamics using universalistic scaling equations, developed in Soft Matter Physics, with a well-defined fundamental reference. They are Super-Malthusian equations and a critical-like scaling. Significantly, the analytic population dataset, covering the period from the Anthropocene onset to 2025, is examined to determine the newly proposed analytic per capita relative growth rate (RGR), which is then used to ultimately validate the scaling equations discussed via RGR-based, linearized, distortion-sensitive analysis. Notably, the discussion focuses on basic patterns in the dynamics of Soft Matter systems and also indicates some parallels to the nuclear chain reaction pattern. The report also discusses emerging links between significant ecological and historical events and characteristic changes detected in global population evolution.

Keywords: Active Soft Matter; Global Human Population; Dynamics; Scaling; Critical behavior; Stretched exponential; Compressed exponential; Carrying Capacity

1. Introduction

Today, there are 8.3 billion people on Earth, with a daily increase of ~150,000 infants. Determining changes in the global population through 2100 is crucial for global planning and management across many areas, including politics, food security, critical raw materials, and ecology (WPR, 2026; Taagapera & Nemčok, 2024; Sojecka, Drozd-Rzoska & Rzoska, 2024; Sojecka, Drozd-Rzoska & Rzoska, 2025). This is predominantly determined by the universal metric of Global Carrying Capacity (Sojecka, Drozd-Rzoska & Rzoska, 2025). However, reliable predictions require a sound understanding of the past. The importance of such past experiences was perhaps first emphasized in the Holy Bible: the phrase from *Ecclesiastes I, 10* "*nihil novum sub sole*", (*there is nothing new under the sun*), then repeatedly invoked in various forms by thinkers.

For the authors particularly notable is Cicero .(106 BC to 43 BC, Ancient Roman Republic times), who specified (Everitt,2003): '*Historia vero testis temporum, lux veritatis, vita memoriae, magistra vitae, nuntia vetustatis, qua voce alia nisi oratoris immortalitati commendatur?* (eng.: *By what other voice than that of the orator is history, the true witness of times, the light of truth, the life of memory, the mistress of life, the heraldress of antiquity, committed to immortality?*).

Therefore, let us use this guideline to attempt to estimate future changes in the global population and the associated changes in global carrying capacity. Let us look back on past experience, dating back to the origins of the human population. However, the aim of this study is to provide insight grounded in the principles of the Scientific Method (Holman, 2023; Harper, 2012), in which empirical data and the clear validation of the models used to describe them are paramount. In this paper, we present an analysis of both the global population and the global Carrying Capacity.

The authors of the given report implement this essential rule by using the dynamics of (Human Intelligent, HI) Active Soft Matter concept as a reference, for discussing global population changes. This provides an explicitly universalistic, in-depth, and validated fundamental basis. This report summarizes the authors' research in these directions and presents new interpretations and results, particularly regarding Global Carrying Capacity, supplemented by new concepts and reasoning.

However, before we begin, it is necessary to indicate and justify the starting point of the history of the global human population discussed in this report.

A decade ago, pre-human footprints were discovered in western Crete (Greece). They show hominin-like features and date back to the late Miocene. ~5.7 million years ago (Gierliński et al., 2017). After long evolutionary development and population growth, Human ancestors in Africa and Eurasia were pushed to the brink of extinction around 900,000 years ago (Grine & Fleagle, 2009; Hu et al., 2023). About 98.7% of human ancestors were lost. This was supported by genetic tests of the fossil record from Africa and Eurasia, which date to between 950,000 and 650,000 years ago. This extremely small population, likely only 1,200–1,500 individuals, is the ancestor of all subsequent human populations (Hu et al., 2023). Not only did they survive successive long periods of global glaciation, interrupted by shorter interglacial warmings, but they also reached locations on almost all continents — Antarctica being the obvious exception. Remarkably, this progress was achieved during the last glaciation, which was perhaps the most severe in terms of climate. This can only be attributed to an increasingly evolved ability to adapt and utilize all available environmental resources, often scarce, at a given level of development. The undoubted advantage of the genus 'Homo' was adaptive intelligence, supported by social interactions.

The first anatomically 'modern' Homo Sapiens appeared in Africa around 300,000 years ago. The oldest known remains were discovered at Jebel Irhoud in Morocco. This occurred during one of the previous Ice Ages, which lasted over 50,000 years. After a brief interglacial period, however, the next Ice Ages followed. They culminated in a particularly long and severe last Ice Age that peaked only 20,000 years ago. However, as early as 19,000 years ago, a period of rapid warming known as the 'Great Thaw' began (Grine & Fleagle, 2009; Ehlers & Gibbard, 2007).

This interglacial period continues to this day and was only briefly interrupted by the Younger Dryas episode, which peaked 11,700 years ago. This also marked the beginning of the Holocene, which continues to this day. This period is associated with the rapid development of Homo sapiens and the beginning of the Anthropocene era, which is linked to 10,000 BCE. The end of the Ice Age and the subsequent Global Warming sped up so rapidly that, by 16,000 years ago, the ice sheets in Europe had retreated to the Alps, Scotland, and the region stretching from Scandinavia to the northern coast of Poland and the Baltic states. In America, meanwhile, the ice sheet had already begun to retreat northwards along the western coast of North America, leaving a wide, clear corridor. However, the ice sheet was still relatively close to the ocean floor, meaning its level was around 100 meters lower than it is today (Ehlers & Gibbard, 2007).

This meant there were wide land passages from Asia to the Americas via the Bering Strait. The continental nature of Great Britain and Ireland was such that they were almost connected to Scandinavia by the 'Grand Doggerland', which extended beyond the North Sea. The La Manche Channel (English Channel) was also land at that time, of course (Stutz, 2026). In a warming climate, these ice-free areas provided additional opportunities for the growth and development of the Homo sapiens population.

This work analyses global population changes from the beginning of the Anthropocene, when Europe was free of glaciers and North America was experiencing a very rapid glacial retreat. A Brave New World opened up, offering an increasingly favorable climate for humans and unlimited resources within the needs and exploration capabilities of contemporary human populations. The human population had already undergone unique multidimensional evolution during the Ice Ages. It included cognitive abilities and the development and implementation of technological innovations that were passed down and further refined in subsequent generations. Perhaps most important were increasingly sophisticated social and cultural relationships.

2. Standard approaches to the global population dynamics problem

First, we would like to revisit the general overview of global population change in the Anthropocene, as depicted in the standard picture provided by the United Nations Population Fund (UNESA, 2026; UNFPA, 2026), and shown in **Figure 1**. In particular, they highlight the Neolithic period in the prehistoric era, when the population was at its terminal stage. They also indicate the Roman Empire epoch in late Antiquity.

It is worth noting the unique, complex, dynamic system features of the global population:

(i) Global Population is a ‚closed', Planetary System
(ii) External impacts are minimal: the last grant planetary extinction due to the Chicxulub Asteroid impact, near the Yucatan Peninsula, occurred 66 million years ago
(iii) It is governed and driven only by internal features and dynamics
(iv) There is no external population's impact *(*assuming UFOs, Aliens, etc, do not exist*)*

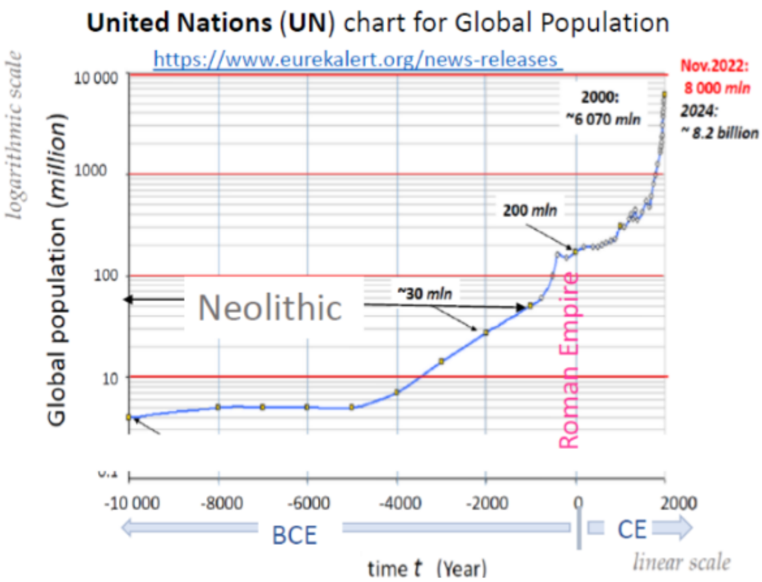

Figure 1.: The picture standard of the United Nations, with the authors' supplementation to indicate issues significant to the given report (UNESA, 2026; UNFPA, 2026).

Regarding human population growth modelling, there are two standard cognitives:
1st Path, probably dominant, aims to define the Global Population via impacts of geographical regions, social groups, education, multiple social interactions - especially the role of women, migration, education, birth/death ratio, age structure, economic development... Such a multitude of data is analyzed statistically via models developed in management, econometrics, bio-evolution, or socio-economic sciences. (Ribeiro, 2017; Kendall et al., 2011; Lima & Berryman, 2011; Cecconi et al., 2012; Kac & Lutz, 2017; Vollset et al., 2018; Dias et al. 2018; Herrington, 2020; Bystroff, 2021; van Witteloostuijn et al., 2022; McFarlane, 2023; Raftery & Ševčíková, 2023; Hill et al., 2011; Shumway & Stoffer, 2017; Dai J, Chen , 2019).
2nd Path, is related to creating a convincing model scaling equation, which subsequently is used for portraying the population data in a selected time period. (Malthus, 1798; Stokstad, 2005; Katul, 2013; Verhulst, 1847; Yumei, et al., 2007, Bacaër, 2008; Zhan, 2008; Kapitza, 2010; Lima & Berryman, 2011; Iannelli & Pugliese, 2014; Siegel, 2015; Gonzalo & Alfonseca, 2016; Flies et al., 2018; Keilman, 2020; Gu et al., 2021; Lehman, 2021; Narayan et al., 2022; Taagapera & Nemčok, 2023; Lima, 2024; Espinosa & Koh, 2024; Lam, 2024; Taagapera & Nemčok, 2024).

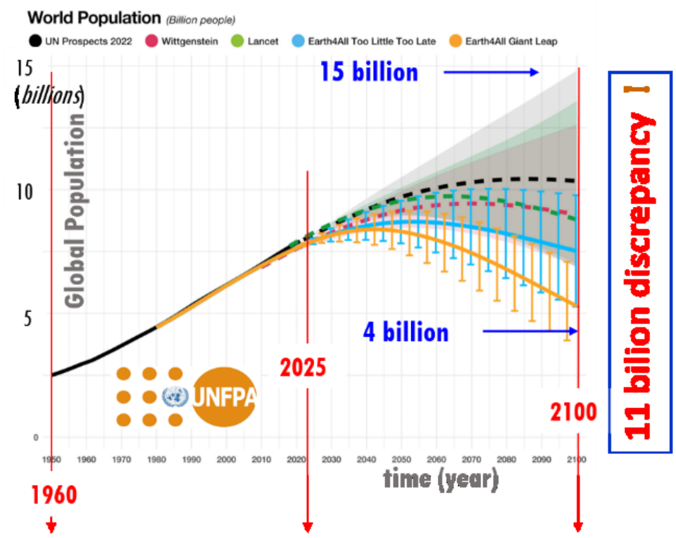

Figure 2. The United Nations Population Fund (UNFPA) standard, with the authors' supplementation, presents forecasts of global population changes until 2100 using **1st Path** modelling. The plot is based on data from 1950 to 2022, and, of course, reproduces the changes well. Then, discrepancies appear, reaching as much as 11 billion in 2100 (UNFPA, 2026).

Figure 2 illustrates the essence of the **1st Path** - related results, via the official UNPFA chart (UNFPA, 2026). Notable is the scatter in forecasts, reaching almost 11 billion (!) for 2100. This puzzling result can be explained by the following issues inherently associated with this cognitive path:

(i) A multitude of ‘empirical’ data that have to be collected from many scattered sources. The types of these parameter series chosen often depend on the conceptual preferences of the authors of a given analysis.

(ii) The meaning and interplay of the above multitude of data series require 'weighting factors', which are necessarily burdened by the arbitrariness of 'experts' opinions. Furthermore, these factors must, or at least should, be considered in the context of the time in which they are introduced, and in light of the often qualitatively different social and cultural conditions across different parts of the globe.

(iii) The multidimensional, essentially iterative, analyses of global population change are carried out by implementing concepts from various fields of natural and cognitive sciences, with the impact of the model's underlying assumptions.

(iv) The above points lead to the challenge of reliably determining the uncertainty of the results.

(v) The required series of precise data are available only after 1950 (UNFPA, 2026; UNESA, 2026).

The **2nd Path** in global population dynamics modelling dates back to the pioneering work of Thomas Malthus. He was inspired by the great legacy of Isaac Newton, who demonstrated in practice the extraordinary power of the Scientific Method and the belief that there are universal laws of nature connecting various, seemingly separate phenomena, which can be represented by universal scaling relations. Notably, to highlight model interpretations, Newton developed and implemented differential calculus. Thomas Malthus, following heuristic considerations, proposed the following model equation to describe population changes (Malthus, 1798; Stokstad, 2005; Katul, 2013):

$$P(t) = P_0 \exp(rt) \Rightarrow \ln P(t) = \ln P_0 + rt \quad \Rightarrow \frac{\mathrm{d}P(t)}{\mathrm{d}t} = rP(t), \tag{1}$$

where time t refers to the onset time t_0, coupled to the prefactor P_0, and $r = const$ is the Malthus rate coefficient.

The middle part of Eq. (1) defines the Malthus model validation via the linear pattern in the plot $\ln P(t)$ vs. time t. Malthus (1798) supplemented bythe heuristic assumption for a much weaker growth of necessary resources, originally food, approximated via a linear dependence (Malthus, 1798):

$$F(t) = a + bt. \tag{2}$$

Probably, this relation resulted from Malthus's current observations that increasing food resources require a proportional rise in the size of cultivated fields. Malthus concluded (Malthus, 1798): '*The population increases in geometrical ratio and the subsistence rises only linearly, which finally leads to times of vice and misery*'. Finally, this is the Malthusian Trap (Catastrophe) (Malthus, 1798; Stokstad, 2005; Katul, 2013), when the quantity of food becomes increasingly insufficient to support the growing population. Malthus advised population self-constraints or an additional rise in subsistence (food) to escape the catastrophic Trap (Malthus, 1798). Unfortunately, the primitive escape concept, such as robbery or conquest of other countries, has often been implemented by rulers or politicians to ‚solve the problem'.

In the mid-19th century, Verhulst proposed the next model scaling equation, which inherently includes the impact of resources available in the system (Verhulst, 1847; Pearl & Reed, 1920; Pearl, 1927):

$$\frac{\mathrm{d}P(t)}{\mathrm{d}t} = rP - sP^2 = P(r - sP) \quad \Rightarrow \quad \frac{\mathrm{d}P(t)}{\mathrm{d}t} = rP\left(1 - \frac{P}{r/s}\right) = rP\left(1 - \frac{P}{K}\right) \tag{3}$$

$$P(t) = \frac{P_0 \exp(rt)}{1 + (P_0/K)(1 - \exp(rt))} \Rightarrow (s \to 0,\ K \to \infty) \quad \Rightarrow \quad P(t) = P_0 \exp(rt), \tag{4}$$

where r means the Malthus growth rate, s is the resources (originally food) factor, the carrying capacity $K = r/s$, and $C = P_0/(K - P_0)$.

The left-hand part of Eq.(3) is for the original Verhulst notation (Verhulst, 1847), and the right one is for the reformulation by Pearl & Reed (Pearl & Reed, 1920; Pearl, 1927), who introduced the Carrying Capacity factor (K), now one of the most significant concepts in discussions on sustainable development and ecological issues. Following Eq. (3), it indicates the maximal population allowed for sustainable coexistence with the environment in a given system, i.e., $K = P_{\max}^{\text{sustain.}}$. The right-hand part of Eq. (3) shows the terminal approximation leading to the basic Malthus dependence.

Notably, when taking into account the Taylor expansion, Eq. (3) can be s extended to the following form

$$\frac{\mathrm{d}P(t)}{\mathrm{d}t} = rP\left(1 - 1 + \frac{P}{K}\right) \approx -rP(t)\ \ln\left(\frac{P}{K}\right), \tag{5}$$

which correlates with the so-called Gompertz equation (Yumei et al. 2007), also used in population studies.

Worth noting are some problems that can be noted for the **2nd Path** implementations carried out so far.

In general, the basic Malthus, Verhulst, or Gompertz (Yumei et al. 2007) equations do not accurately reproduce global population changes. However, they are significant tools for describing different population dynamics in biology, medicine, and food technology. When considering the results of such analyses, it is worth noting some general issues. In physics, where nonlinear fitting with scaling functions is an extremely common, even routine, way of data analysis, it is widely assumed that optimal and reliable results require 10x as many experimental points as the number of fitted parameters in a given model equation.

(i) The Malthus relation contains only 2 free parameters that can be determined by linear regression for a straight line, which, by definition, gives reliable and optimal values, along with errors

(ii) Verhulst and Gompertz relations for $P(t)$ changes contain 3 free parameters, and here nonlinear fittings are typically

(iii) Numerous 'extension' models, for which the Verhulst and Gompertz equations are the limiting reference, introduce 4, 5, or more parameters.

(iv) Especially for the latter two cases, the quality of fit should not be assessed by 'satisfactorily' portraying empirical data or by providing the associated 'favorable' parameters describing the quality of fit (R^2, χ^2, ...). The actual errors in the fitted parameters will be extremely unfavorable, even exceeding 50% of their values. This is due to the very flat minima of the individual fits for these parameters – meaning that even a significant change in their values will not affect the 'visual' quality of the fit.

Notably, recently Lehman et al. (2021) considered global population growth using an extended Verhulst model that takes into account three successive bio-ecological levels: (a) interactions with predators, (b) interactions with prey, and (c) intraspecific interactions. Global population changes at each level are governed by level-dependent ecological coefficients $(r_i;\ s_i)$, $i = 1;2;3$. These were implemented for the following extended Verhulst-type equations (Lehman et al,2021):

$$G_P = \frac{1}{P(t)}\frac{\Delta P(t)}{\Delta t} = r_i \pm s_i P(t) \qquad \Rightarrow \qquad P(t) = \sum \frac{1}{\left(P_0 \mp (s_i/r_i)\mathrm{e}^{-r_i t} \pm (s_i/r_i)\right)} \ , \tag{6}$$

where coefficients $r_i, s_i = \mathrm{const}$, for subsequent time domains differently subjected to time-varying bio-/eco- factors. G_P denotes the Relative Growth Rate(RGR), in a commonly used discrete form,

For the empirical validation of the multiparameter Verhulst approach Lehman et al. showed the linear behavior of $G_P(P_i)$ vs. $P_i(t_i)$, in two domains, namely from 10 000 BC to ~1962 and next from 1869 to 2019, using 98 population data coveting this Anthropocene period. The mentioned crossover was associated with $P(t_{\mathrm{cross}}) \approx 3.14 \pm 0.2$ billion (Lehman et al., 2021). However, the enormous time span of 12 millennia, combined with the colossal population change, results in a very 'squeezed' presentation at terminals. The latter can bias the RGR validation tests, as shown very recently in ref. (Sojecka & Drozd-Rzoska, 2025).

In 1960, von Foerster et al. (1960) suggested a possible preference for a qualitatively different scaling function than previously discussed. It was later referred to as 'Hyperbolic' or 'Doomsday' scaling. Global population data, covering a period of 1500 years from 400 CE to 1958, were scaled by the following function (von Foerster et al., 1960):

$$P(t) = \frac{A}{(D-t)^M} \approx \frac{A}{D-t} \qquad \Rightarrow \qquad \log_{10} P(t) = \log_{10} C - M\ \log(D-t)\ , \tag{7}$$

where $C = (1.79\ \pm 0.14) \times 10^{11}$ (years), the exponent $M = 0.99 \pm 0.01$, $D = 2026.87 \pm 5.5$ (years) which was linked to the fate 'Doomsday' on Friday, 13th Nov., 2026 in the title of (von Foerster et al., 2026).

The right-hand part of Eq. (7) defines the log-log scale analysis, with an adjustable 'Doomsday' parameter D, until reaching the linear pattern used in (von Foerster et al., 1960). This result is recalled in **Figure 3**.

Nonetheless, von Foerster et al., (1960) met extensive criticism soon after the publication. However, the objections were rather general and speculative, primarily concerning the 'strange' Doomsday singularity predicted for late 2026, noted as 'artificial' and without any real meaning. The next ones were related to no underlying model (Shinbrot, 1961; Roberstson et al, 1961; Hutton, et al, 1961; Howland, 1961; Serrina, 1975; von Hoerner, 1975;

Smith, 1977; Podum E, Whither, 1980; Umpleby, 1987; Deevay, 1988; Frasere-Smith, 1989; Kremer, 1990; Dochy, 1995; Hough, 1996; Varfolomeyev et al, 2001; Umpleby, 2005; MacIntyre, 2005; Dolgonosov & Naidenov, 2006). Till the mid-1970s, as more historical estimates of the global population have become available, evidence showing different values for the exponent in the 'Doomsday' Eq. (2), $0.7 \leq M \leq 1$. Moreover, it was noted that parameters obtained in scaling via Eq. (7) depended on the selected time domain (Kremer, 1990; Dolgonosov & Naidenov, 2006).

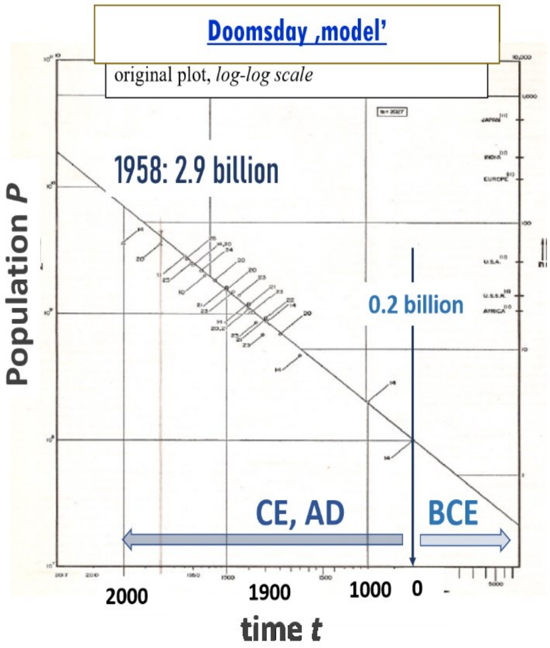

Figure 3. The original plot by von Foerster et al. showing global population changes from over 1500 years, to 1958 via the log – log scale analysis validating the 'hyperbolic' scaling, as shown in Eq. (7) (von Foerster et al., 1960). The plot includes supplements by the authors of the given report to facilitate reading.

The analysis by (von Foerster et al., 1960) used the $\log_{10}P(t)$ vs $\log(D-t)$ plot, with adjustable D value until obtaining the linear behaviour. However, the huge distance between the terminal of the tested empirical data and the singularity means that even relatively large changes in the value of D are poorly detectable. This problem was explicitly demonstrated in studies of the pseudospinodal behavior in near-critical liquids (Chrapeć et al, 1987).

When discussing the above scaling concept, worth recalling is the model picture by Taagapera and Nemcok (Taagapera & Nemčok, 2023; Taagapera & Nemčok, 2024), who focused on a scaling equation that correlates with the 'Doomsday' scaling in a 'remote, tail' domain. It led to the 'tamed quasi-hyperbolic function', or 'T-function' (Taagepera, 1977; Taagapera & Nemčok, 2023; Taagapera & Nemčok, 2024):

$$P(t) = \frac{A}{[\ln(B+E)]^M} \quad , \quad \text{where } E = \exp[(D-t)/\tau] \ . \tag{8}$$

They showed a fair portrayal for two subsequent periods (1) from well below 10 000 BCE to 400 CE and (2) from 400 CE to 2022. Both domains terminated with a plateau, namely during Roman Empire times and in the last decades, up to 2022, which might suggest universalistic population terminals and the split into two leading (civilizational?) periods in the Anthropocene. A worth stressing result of refs. (Taagapera & Nemčok, 2023; Taagapera & Nemčok, 2024) is the presentation of ~ 600 collected global population data, showing significant discrepancies in estimates, which increase when shifting back in time. However, it is notable that Eq. (8) contains 5 nonlinearly fitted parameters, which makes ultimate validation difficult.

3. Global Population: Physics & Active Soft Matter Perspective

To date, studies of global population change have paid (very) limited attention to the patterns offered by the dynamics of complex systems in physics, despite their explicit, fundamental interpretative basis, which is often empirically tested and validated. Only recently, the authors of this report followed this **3rd Path** for global population growth cognition (Sojecka Drozd-Rzoska &Rzoska, 2025; Sojecka & Drozd-Rzoska, 2025; Sojecka & Drozd-Rzoska, 2024; Sojecka & Drozd-Rzoska (Proc. Socr. Lect.), 2025; Sojecka & Drozd-Rzoska, 2023; Sojecka & Drozd-Rzoska, 2026). These issues are presented in detail in the next section, alongside new and previously unpublished analyses. Dynamical processes involving exponential changes, i.e., resembling the Malthus equation, are relatively common in physics. An example is the dynamics of a nuclear chain reaction, which will be discussed in reference to the basic 'standard' population scaling patterns in the next section. More complex dynamics emerging in the global population are discussed within the framework of complex Soft Matter dynamics in subsequent sections.

3.1 Malthus scaling, Verhulst scaling, and the nuclear chain reaction parallel

In this section, we would like to draw your attention to an almost direct parallel with a process that is well known, at least by name: the nuclear chain reaction. However, neither Malthus's nor Verhulst's equations have been invoked there, so far. The nuclear chain reaction is related to a cascading increase in neutron emission, namely (Cameron, 2011):

$$\frac{\mathrm{d}N(t)}{\mathrm{d}t} = \left(\frac{k_{\mathrm{eff}} - 1}{l}\right) N(t) \qquad \Rightarrow \qquad \frac{\mathrm{d}P(t)}{\mathrm{d}t} = rP(t) \tag{9}$$

where the left side is for the neutron population and the right side evokes Malthus's relation for the populations of humans, animals, bacteria, or yeast. The effective neutron multiplication factor is defined on the left side of the relation below (Cameron, 2011):

$$k_{\mathrm{eff}} = \frac{\text{rate of neutrons production}}{\text{rate of neutrons loss}} \qquad \Rightarrow \qquad k_{\mathrm{eff}}^{\text{popul.}} = \frac{\text{birth rate}}{\text{death rate}} \ . \tag{10}$$

The right-hand side is for the possible human/species population changes.

In a nuclear chain reaction, the prompt-neutron lifetime refers to the time it takes for a neutron to undergo fission. For human populations, the parameter l can also be associated with the life-time, most often too prompt, unfortunately. Following the above, one obtains for the meaning of the Malthus growth rate:

$$r = \frac{k_{\mathrm{eff}}^{\text{popul.}} - 1}{l} \qquad \Rightarrow \qquad \tau = \frac{1}{r} = \frac{l}{k_{\mathrm{eff}}^{\text{popul.}} - 1} \qquad \Rightarrow \qquad P(t) = P_0 \exp\left(\frac{t}{\tau}\right) \ , \tag{11}$$

where the right-hand part shows the formulation of the Malthus relation using the relaxation time τ, as proposed in ref. (Sojecka & Drozd-Rzoska, 2024) Such notation, commonly used in physics, enables a simple estimation of the time required to 50% change in population: $t_{50\%} = \tau \times \ln 2$.

For the nuclear chain reaction, three main domains for the effective neutron multiplication factor, which can be directly implemented in the Malthus model population analysis (Cameron, 2011):

(i) $k_{\mathrm{eff}}, k_{\mathrm{eff}}^{\text{popul.}} < 1$ ('<u>subcriticality</u>'): the population is decreasing exponentially

(ii) $k_{\mathrm{eff}}, k_{\mathrm{eff}}^{\text{popul.}} = 1$ ('<u>criticality</u>'): the population is maintaining a constant value

(iii) $k_{\mathrm{eff}}, k_{\mathrm{eff}}^{\text{popul.}} = 1$ ('<u>supercriticality</u>'): the population is increasing exponentially

In a practical nuclear system, like a fission reactor, k_{eff} oscillate from slightly less than 1 to slightly more than 1. When permanently $k_{\mathrm{eff}} > 1$ or even $k_{\mathrm{eff}} \gg 1$, there is a danger of a nuclear explosion, with gigantic destructive force: 'Atomic Bomb' explosion.

The latter could be a fundamental justification for the concept of the 'Demographic Bomb', often used in global population studies, in connection with possible values $k_{\mathrm{eff}}^{\text{popul.}} \gg 1$.

For nuclear power plant operation, it is essential to maintain a constant, near-critical electron emission rate without actually reaching a critical or supercritical k_{eff} value, which could lead to an uncontrolled nuclear reaction. This is achieved by immersing the fuel rods in a suitable medium, such as heavy water (D_2O), which slows down neutrons and limits the nuclear chain reaction to a predetermined level. This process is described by the neutron population equation (NPE) (Cameron, 2011):

$$\frac{\mathrm{d}N(t)}{\mathrm{d}t} = \left(\frac{k_{\mathrm{eff}} - 1}{l}\right) N(t) + S(t) = k_{\mathrm{Neu}} N(t) + S(t) \ , \tag{12}$$

where $S(t)$ describes the influence of the medium in which the fuel rods are immersed. until reaching a state where $\mathrm{d}N(t)/\mathrm{d}t \to 0$, when the appropriate neutron population stops growing, but their stable 'effectively subcritical' emission ensures constant production of thermal and further electrical energy.

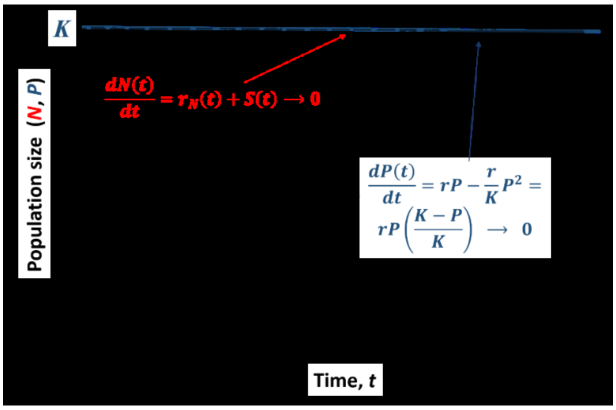

Figure 4. Bimodal pattern, consisting of the rising and stationary parts, with recalling the neutron population equation for: **(1)** power plants (in red) and **(2)** the Verhulst equation for human or any other bio-population (in blue). The latter includes the Carrying Capacity factor (K), also indicated in the plot. Arrows indicate the final, stationary population value.

Both in the NPE Eq. (12) and in the Verhulst Eq. (3), a supplementary term describing 'environment' features significant for the given population is included. Generally, $S(t)$ factor is specified with respect to the nuclear reactor implementation. On the other hand, the Verhulst scaling equation, associated with human or bio-populations, assumes a simple pattern for such a term: $S(t) = (r/K)P^2$, showing explicitly the dependence from the population $P(t)$ size, growth rate and maximal, final and sustainable population.

For the Verhulst Eq. (3), the bimodal pattern shown in **Figure 4** is a standard for bacterial populations in a closed container, where the essential feature of the environment is that the food resource is constantly replenished to a constant level despite its consumption by the growing population. For a nuclear reactor, the meaning of 'resource', in the given case the moderated medium, is different, namely limiting quantitative changes in the 'electron population' to a critical level (the **A**-case above), essential for reaching the second 'stationary' state in **Figure 4**. This may indicate the Verhulst model's usefulness in nuclear reactor modelling. The authors believe that the direct implementation of the Carrying Capacity (K - factor) concept as a universal metric for environmental capacity relative to the needs/requirements of a given population may be particularly valuable here.

3.2 Human Active Intelligent Soft Matter Insight into Global Population Dynamics

In 1991, Pierre G. de Gennes presented the Nobel Prize Lecture entitled (de Gennes & Badoz, 1996): 'Soft Matter'. It introduced the novel category of systems, linking: liquid crystals, polymers, blends, gels, foams, supercooled glass-formers, colloids, critical liquids … and bio-systems. Soft Matter complex systems exhibit a few common features:

(i) dominance of mesoscale species leading to ‚universal' scaling patterns of ‚isomorphic' physical properties
(ii) ability to spontaneously self-assemble
(iii) extreme sensitivity to Exo- & Endogenic impacts, linked to weak interactions between mesoscale species

Jones (2002), in his classic monograph indicated four conceptual and cognitive 'pillars' that are essential for interpretation in any Soft Matter framework: (i) Liquid Crystals Physics, (ii) Glass Transition Physics, (iii) Polymers Physics, and (iv) Critical Phenomena Physics.

In subsequent years, the Soft Matter category entered other branches of Science. One can recall Quantum Soft Matter (Thedford, 2023), Cosmological Soft Matter (Saridakis, 2021), Topological Soft Matter (Serra et al, 2020), and, perhaps most important and rapidly developing, Active Soft Matter (ASM) (Menzel, 2015; Das et al, 2020; Janzen, et al, 2026) for complex systems composed of interacting elements that can individually consume energy and then collectively generate motion or mechanical stress.

ASM links Soft Matter physics, biology, and medicine (Tang, 2022; Gonzalez-Rodriguez, et al., 2012) to understand the unique patterns that emerge in systems such as viral assemblies, bacterial colonies (Sawada, 2017) , tissue formation (Gonzalez-Rodriguez, et al., 2012) gene expression (Semerano, et al., 2025) It also explains collective motion observed in bird flocks (Cavagna, et al, 2015), schools of fish (Huang et al, 2024), bee swarms (Shpurov & Froese, 2022), and anthills (Hu, et al., 2016). Very recently, a new subcategory of Intelligent Soft Matter (ISM), that links Active Soft Matter Physics, Biology, & Cognitive Sciences, has emerged (Baulin, et al., 2025; Wrugt, 2026).

This report focuses on the proposal for a new category, Human Active Intelligent Soft Matter (HAI SM). This report explores this concept to gain new insight into global population dynamics since the onset of the Anthropocene. Notable are the model features of HAI SM:

(i) An extraordinary range of adaptation to a 'system' despite environmental changes, food resources, threats, etc...

(ii) Creation of 'innovations', their memorization, improvement, and transfer to the next generations, supporting adaptation to the system, and even shaping it

(iii) The ability to 'hierarchical assembling' targeting on better and more efficient acquisition of food and raw materials, but also on activities related to other 'hierarchically assembled' species, focused on defensive purposes and/or aggressive super-predator activities

(iv) Multidimensional interactions – 'biological', 'ecological' with the environment, but also social. Significant is the rapid development of language, or the development of seemingly 'impractical' actions, indirectly strengthening communities (rituals, religion, art, etc.)

However, before proceeding to the implementation discussion, the authors would like to first draw attention to a specific drawback and limitation in the empirical validation of model scaling relations – the scatter of global population data, illustrated in refs. (Taagapera & Nemčok, 2023; Taagapera & Nemčok, 2024). It means their non-analytic nature, which excludes all methods related to numerical differentiation of empirical data, being the essential path for 'subtle', ultimate, validation tests.

The authors of this paper implemented the following protocol to address this essential challenge (Sojecka & Drozd-Rzoska, 2024; Sojecka & Drozd-Rzoska, 2025):

1. The first step focuses on the empirical data itself, which: (i) are collected from different sources, which gives them a large scatter – a big problem so far, (*ii*) the data are then subjected to numerical filtering (using the Savitzky-Golay principle) – until an 'analytical' set is obtained, which can be directly differentiated
2. The next focus on scaling equations with no more than 3 adjustable parameters, & used in testing dynamics of Soft Matter systems (and not for Global Population studies, so far)
3. Instead of direct fitting, the adequacy of a given scaling relation for describing a given set of 'empirical' data is tested, using the distortion-sensitive & derivative-based analysis
4. The analysis shows time domains of given relation validity and determines optimal values of parameters, and subsequently inserted into the scaling relations for portraying $P(t)$ data.

Figure 5 illustrates changes in the global population, from the Anthropocene onset (10,000 BC) to 2025 (i.e., over 12 millennia), using the dataset prepared following the above protocol. For the first nine millennia, **Figure 5** indicates a simple Malthusian pattern split into two periods corresponding to the Early and Late Neolithic epochs. Notable is the coincidence of the crossover (~5,000 BC) with the early post-final flooding of Doggerland remains. It was the landmass that connected Britain with Scandinavia, yet around 8,000 BC. Nowadays, this region is known as the North Sea, with an average depth of 80 - 90 meters (Stutz, 2026).

From around 1000 BC onwards, the dynamics of the global population, as shown in **Figure 5**, appear to be non-linear and non-Malthusian. However, two specific periods emerge, marked by red horizontal lines, during which the global population barely changed: the

Roman Empire period in late antiquity and the period from late Medieval to th Renaissance, which coincides with the times of Black Death pandemic impact.

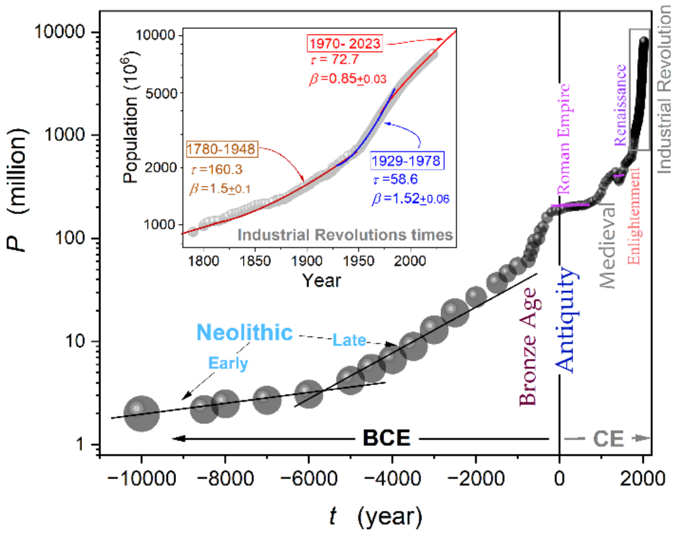

Figure 5. Global population change (200 population data points) obtained through numerical filtering of data from refs. (Sojecka AA, Drozd-Rzoska, 2024; Sojecka AA, Drozd-Rzoska, 2024; Drozd-Rzoska & Sojecka, 2026) in the semi-log scale, for which the ‘simple’ description of Malthus Eq. (1) manifests itself as a domain of linear changes. The inset shows behavior related to the Industrial Revolution period since 1800, parameterized via the empowered exponential relation, the Super Malthus Eq. (14), described above. Some significant periods and dates are indicated.

4. Super Malthusian scaling of Global Population changes

The development of an analytical dataset for the global population changes, by the authors of the given report, led to the proposal of the Analytic relative growth rate (RGR) factor (Sojecka & Drozd-Rzoska, 2025):

$$\left[G_P = \frac{1}{P(t)}\frac{\Delta P(t)}{\Delta t}\right]_{\text{discrete}} \Rightarrow \quad G_P(P,T) \quad = \left[\frac{1}{P(t)}\frac{\mathrm{d}P(t)}{\mathrm{d}t}\right]_{\text{analytic}} \Rightarrow$$

$$\Rightarrow \quad G_P(P,T) \quad = \frac{1}{P(t)} \ \frac{\mathrm{d}P(t)}{\mathrm{d}t} = \frac{\mathrm{d}\ln P(t)}{dt} \tag{13}$$

The analytic RGR, describing relative population changes $\mathrm{d}P(t)/\mathrm{d}t$ along the timeline, has been implemented as a universal testing tool for detecting subtle features of population changes, hidden in the standard $P(t)$ plot view.

Figure 5 shows that, for much of the Anthropocene, global population dynamics is non-Malthusian, i.e., they exceed the simple exponential (‘geometric’) growth defined in Eq. (1). One of the leading methods for scaling this type of empirical data in physics is the empowered exponential function. The authors of this paper implemented such an approach in ref. (Sojecka AA, Drozd-Rzoska, 2024), naming the new scaling function as Super Malthusian (SM):

$$P(t) = P_0 \exp\left(\frac{t}{\tau}\right)^{\beta} \ \Rightarrow \ G_P = \frac{\mathrm{d}\ln P(t)}{\mathrm{d}t} = \frac{\beta}{\tau^{\beta}} t^{\beta-1} = h(t) \ \Rightarrow \ \log_{10} G_P = A + Bx, \tag{14}$$

where $x = \log_{10} t$, $A, B = \text{const}$ and $A = \beta/\tau^{\beta}$, $B = \beta - 1$, and $\tau = 1/r$.

The left-hand side of Eq. (14) defines the SM dependence, and the right-hand side presents the proposed RGR-based linearized distortion-sensitive analysis, to test their validity. Namely, for the plot $\log_{10} G_P$ vs. $\log_{10} t$ linear behavior indicates domains where SM scaling is allowed. Next, linear regression can yield optimal estimates of the relevant parameters with well-defined errors.

The fundamental Soft Matter Physics interpretations of the empowered exponential (Super-Malthus) Eq. (14) (left side) can be concluded as follows:

(i) For the Kohlrausch-Williams-Watts (KWW) model, the exponent $\beta = 1$ is for systems governed by a single relaxation time & $\beta \neq 1$ is for a distribution of relaxation times (Rzoska & Mazur, 2007).

(ii) The most common dynamic associated with $\beta < 1$ is named the stretched exponential, and the case $\beta > 1$ is named the compressed exponential, and it has been only recently evidenced in some physical/material systems (Rzoska et al., 1994; Rzoska et al., 1997; Rzoska & Drozd-Rzoska, 2011; Drozd-Rzoska et al., 2023; Drozd-Rzoska, 2019; Martinez-Garcia, 2013; Wu, 2018; Trachenko, 2021).

(iii) The dynamics governed by for $\beta < 1$ suggest energy loss and $\beta > 1$ energy gain in a system (Rzoska & Mazur, 2007).

(iv) One can also recall the nucleation theory by Avrami, which yields $\beta = D + 1$, where D is for dominant (local) assemblings dimensionality (often fractal) (Rzoska & Mazur, 2007).

The latter, for the human population, can be linked to the emergence of villages, cities, states… The function $h(t)$ in Eq. (14) recalls the Weibull hazard function (Lai, et al, 2006). The Weibull distribution is used extensively in reliability applications to model failure times in complex systems. It is significant for testing failure rates or asset volatility in complex systems with random parameters across various fields, including survival analysis and failure rate modelling. It includes engineering applications for predicting component failure, weather forecasting, and challenging issues in medicine. The hazard function $h(t)$ is telling how likely something is to fail given that it has survived so far. Namely: (*i*) $\beta < 1$ suggests even likely to fall fast, (*ii*) $\beta = 1$ – failure rate is fairly constant, and (*iii*) $\beta > 1$ indicates increasing failure rate as time goes by. (Lai, et al., 2006).

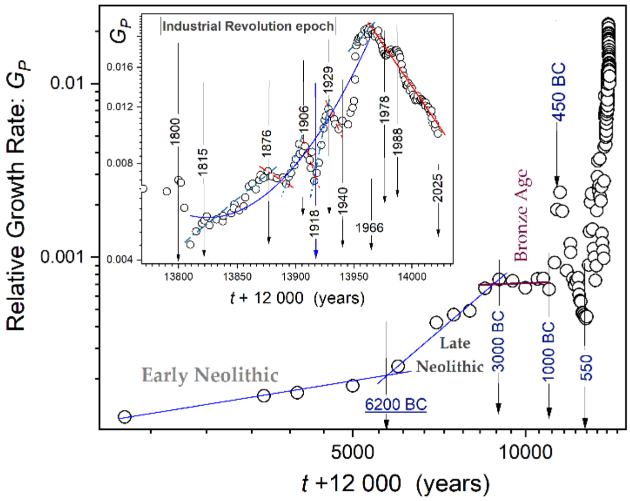

Figure 6. The Relative Growth Rate changes, from the Anthropocene dawn (12 000 BC) till nowadays, in the log-log scale as defined in Eq. (14). The onset present the behaviour focused on industrial Revolutions times, Continuous curves/lines indicate dominant trends and dashed one are for local trends revealed due to the distortions sensitive analysis. The blue and light-blue colours are for the exponent $\beta > 1$ in the Super-Malthus Eq. (14, left part) an the red is for $\beta < 1$. Horizontal lines reflect the basic Malthus pattern related to Eq. (1) or Eq. (14) with the exponent $\beta = 1$.

Figure 6 presents the evolution of the RGR factor on a log-log scale, following the data transformation defined by the right-hand side of Eq. (14), with the slopes of lines directly determining the exponent β. The 'horizontal' behavior is for the basic Malthus pattern (Eq. (1)). It appears in Bronze Age times, for instance. The plot reveals that for Neolithic times, the linear, Malthusian pattern in the direct presentation of $P(t)$ changes has only an 'apparent' meaning. The distortions-sensitive, RGR-related analysis in **Figure 6** shows that it is better described by the SM Eq. (14), within the slightly compressed pattern ($\beta > 1$). Notable is the shift of the crossover between Early and Late Neolithic times to $t \sim 6200\ BC$, which surprisingly well correlates with the sinking' time of the last Doggerland land remnants.

Notably, Bronze Age-related Malthusian behavior fairly coincides with its historical borders (3,000–1,000 BC). This period began with the rise of ancient Sumer in Mesopotamia

and Egypt along the Nile, and ended with the sudden collapse of grand Bronze Age civilizations around 1200–1100 BC. (Glass, 2021).
The times of the Roman Empire (~100 BC – 500 CE) are marked by a pronounced collapse of $G_P(t)$ changes, associated with a remarkable stabilization of the global population $P(t)$ at the level of 190-200 millions for over ~600 years (Garnsey, 2014). This is a unique situation in global population history. A similar disruption, for almost 200 years from ~1350 to ~1540, can be linked to the impact of Black Death pandemic in Asia and Europe (Wickham, 2016; Douglas, 2022).
In searching for RGR collapse during Roman Empire times, the effects of prolonged major wars, the spread of subsequent pandemics through developed communication networks, and significant urbanization can be considered. One can even consider the health effects of lead water pipes. Recently, Sojecka & Drozd (2024) have suggested yet another possible reason for this extraordinary global population collapse: the extraordinary scale of exploitation of "slave work-force"—on a scale we would today describe as "industrial." An example of this deadly exploitation of slaves can be Rio Tinto silver mines in present-day Spain. There was a constant supply of thousands of slaves, who survived for only a few months (Garnsey, 2014). By today's standards, this would be considered organized mass genocide. There were many such places in the Empire, also associated with impressive buildings, which still remains impressive. Notably, at its peak, up to 1/3 of the global population lived in the Roman Empire.
This line of reasoning also raises the question of whether the decline of the Roman Empire was driven by an economic crisis resulting from a shrinking 'barbarian slave workforce' and fewer opportunities to wage victorious wars on its borders.
The inset in **Figure 6** shows a log-log plot of the RGR factor during the ongoing Industrial Revolution era. The global population fluctuations indicated by the arrows in **Figure 6** can be easily correlated with significant historical events, as noted in **Table 1.**

Table 1. Historical events correlated with global population distortions detected in the inset in **Figure 6**.

Year	Related historical facts	Year	Related historical facts
1800	Napoleon Bonaparte terminated the post-Revolution disorder	**1940**	In years (1939-1941), World War II (WWII) spread across the globe
1815	The Vienna Congress established a 'new order' for the next century: the 'concert of powers'	**1950**	The end of post-WWII recovery in Europe, and the onset of a new path of development
1876	The terminal of post-Civil War recovery in the USA - the beginning of the global imperial path; the rise of the German Empire as a new economic and political power	**1966**	The years 1966–1970 were marked by great social upheaval, leading to the transformations that would transform society in the following decades. Also, the 'main wave' of decolonization
1906	Political unrest leading to a modest democratization of the post-feudal Empires, particularly disruptive for Russia	**1978**	The growing economic crises that led to the presidency and reforms of Ronald Reagan in the USA and Margaret Thatcher in the UK
1918	The end 1st World War	**1988**	The communist system collapsed: free elections in Poland (1989), reunification of Germany (1990)
1929	The onset of the Great Economic Crisis: Black Friday		

Drozd-Rzoska & Sojecka (2024) also proposed yet another Super-Malthus equation (named type 2), with the time-dependent relaxation time or alternatively the growth rate:

$$P(t) = P_0 \exp(t/\tau(t)) \quad \Rightarrow \quad \tau(t)=t \ln(P_0/P(t)), \tag{15}$$

where the time-dependent relaxation time can be linked to the time-dependent growth rate as follows: $\tau(t)=1/r(t)$.
The basic problem in applying the above equation for portraying empirical data is the unknown a priori form $\tau(t)$ evolution. However, this problem can be overcome by determining the changes in the relaxation time via the dependence indicated on the right-hand side of Eq. (15).
Figure 7 shows such a result for times after the collapse of the Roman Empire. The analysis reveals two surprising results. Firstly, a dominant basic Malthusian scaling pattern emerges (see Eq. (1)) from the High Middle Ages (~1100) to the onset of the Enlightenment

or the Industrial Revolution (~1700) appears, but with a significant disturbance during Black Death impact times.

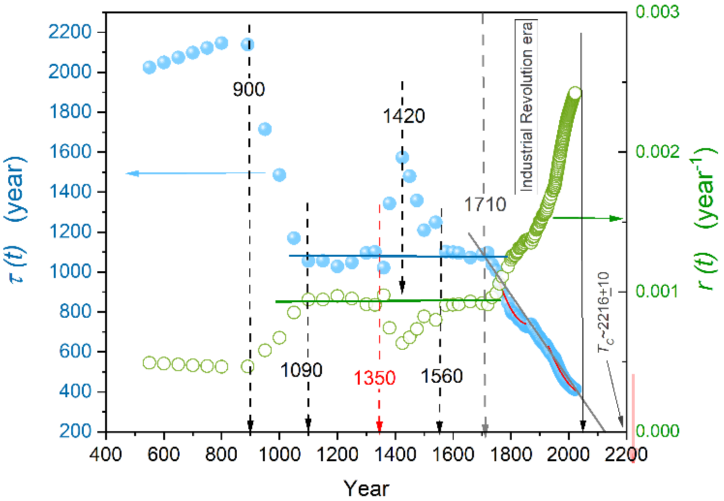

Figure 7. Temporal changes of the relaxation time and the growth rate, $\tau(t) = 1/r(t)$, from the collapse of the Roman Empire to the present day. The dashed vertical arrows indicate the onset of characteristic changes in the plot, with the red arrow corresponding to the onset of the Black Death pandemic. Horizontal lines show the behaviour associated with the dominant trend $\tau(t) = \tau =$ const, related to the basic Malthus behaviour (Eq. (1)), indicated via **green** and **blue** horizontal lines. The sloped, (**grey**) line indicates the dominant linear trend $\tau(t) = a - bT$ in Industrial Revolutions era. Notably, there are two distortions, portrayed in **red** via the second-order polynomial: (1) for years 1970 -2025, and (2) a notably stronger one in years 1780-1860.

In Industrial Revolution time the exceptional linear pattern emerges: $\tau(t) = a - bt$.
In the last few decades. This pattern is disturbed, in a way suggesting 'slowing down in the last few decades. It is indicated by the fitted 'red curve' in **Figure 7**. However, such behavior– in fact, even stronger – also occurred from ~1780 to ~1860, and subsequently the dominant linear trend returned.
Considering the mentioned linear trend as the dominant pattern, one can substitute the related dependence to Eq. (15) (Drozd-Rzoska & Sojecka, 2024):

$$P(t) = P_0 \exp\left(\frac{t}{\tau(t)}\right) = P_0 \exp\left(\frac{t}{a-bt}\right) = P_0 \exp\left(\frac{t/b}{a/b-t}\right) = P_0 \exp\left(\frac{b' \times t}{t_C - t}\right) , \tag{16}$$

where $b' = 1/b \approx 1.62$, $t_C = a/b = 2216 \pm 10$ (year).
Notably, the above relation resembles the constrained critical behavior within the so-called Griffiths model (Drozd-Rzoska & Sojecka, 2024; Amaral & de Oliveira, 2021).

5. Global population – Critical phenomena approach

The second type of scaling relation, which is particularly characteristic, can be associated with the pioneering work of von Foerster et al. (1960), which suggested a hyperbolic scaling relation that was extremely simple yet surprisingly effective. This relation is also known as the 'Doomsday' equation, which predicted an infinite population by late 2026. This was considered a paradoxical result for a random and meaningless date, as seen in the sixties and seventies. Notwithstanding, von Foerster et al. (1960) result inspired further research, although the idea of an explicit (simple) 'hyperbolic' scaling was rejected.
Below, we demonstrate that despite these objections, it is the real dominant trend, but only during the Industrial Revolution era. One can consider von Foerster scaling within the framework of Critical Phenomena Physics (Stanley, 1989).

$$P(t) = \frac{C}{|t_C - t|^M} \quad \Rightarrow \quad \ln P(t) = \ln C - M \ln(D - t), \tag{17}$$

where the critical year t_C can coincide with von Foerster et al. (1960) 'Doomsday' D.
Generally, on approaching the critical singularity the exceptional near-critical (super-critical) state emerges. It is governed by rising multi-element fluctuations, causing the

system to become extremely sensitive to any perturbation. The right-hand part of Eq. (17) recalls the quasi-nonlinear analysis , which employs the log-log plot with an adjustable parameter D, until linear behavior emerges. In fact, it was used by von Foerster et al. (1960). Unfortunately, this type of analysis, as well as the explicitly nonlinear fit, leads to a large uncertainty in the value of the singularity D, also influencing the exponent M. This is due to the significant distance between the singularity and the empirical data terminal. In ref. (von Foerster et al.,1960), they are $D = 2026$ and $t_{\text{terminal}} = 1958$. This also constitutes an unsolved challenge for the analysis of empirical data in physics. One can recall the pseudospinodal problem (Chrapeć, 1987), or dynamics in the high-temperature region of glass-forming systems (Mallamace et al., 2010; Drozd-Rzoska & Rzoska, Starzonek, 2023), for example.

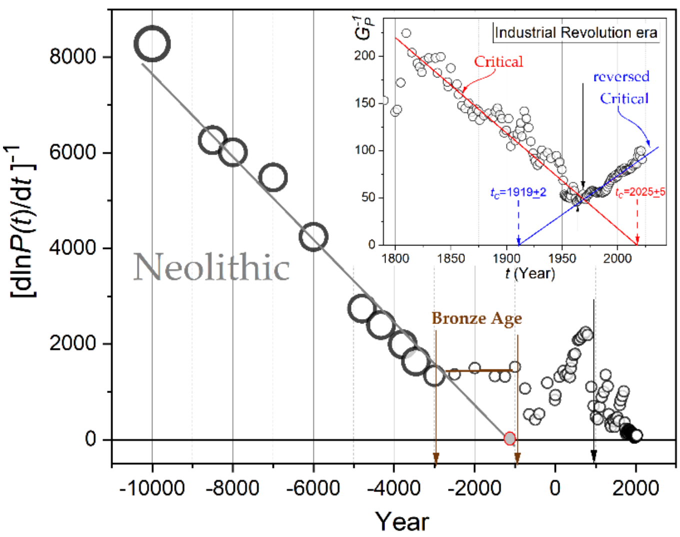

Figure 8. Temporal changes of the RGR factor in Anthropocene, focused on the distortions-sensitive test of the critical-like Eq. (18), with population data transformation defined by Eq. (19). The sloped linear behavior indicates domains where the critical-like Eq. (18) offers a fair scaling. The horizontal line indicates the basic Malthus scaling domain. The inset shows the focused behavior for the Industrial Revolution era. Dashed arrows and the red-border circle indicate singularities t_C for Eq. (18) scaling relation.

The authors of this paper proposed a solution to this problem, namely, recalling Eq. (17) (Drozd-Rzoska & Sojecka , 2026):

$$\ln P(t) = \ln C - M\ln|t_C - t| \quad \Rightarrow \quad \frac{d\ln P(t)}{dt} = \frac{-M}{D-t} \quad \Rightarrow \quad G_P^{-1}(t) = \left[\frac{d\ln P(t)}{\mathrm{d}t}\right]^{-1} \Rightarrow$$

$$\Rightarrow \quad G_P^{-1}(t) = \ -M^{-1}t_C - M^{-1}t = d - mt \ . \tag{18}$$

The implementation of $P(t)$ data transformation defined by Eq. (19) is shown in **Figure 8**. The most striking behavior appears for the Industrial Revolution era, shown in the inset. It reveals the following exceptional sequence (Drozd-Rzoska & Sojecka , 2026):

$$\sim 1800 \quad \rightarrow \quad (D_1 - t)^{M=-1} \quad \Rightarrow \quad \sim 1968 \quad \Rightarrow \quad [\ (t - D_2)^{M=-1}]^{-1} = \quad (t - D_2)^{M=1.1}, \tag{19}$$

where $D_1 \sim\ 2025$, and $D_2 \sim 1919$, for two detected critical ($t_C = D$) singularities It means the following pattern Drozd-Rzoska & Sojecka , 2026):

$$\sim 1800 \quad \rightarrow \quad \text{critical behavior} \quad \Rightarrow \quad \sim 1968(\pm 4) \quad \Rightarrow \quad \text{reversed critical behavior} \tag{20}$$

The first 'critical' domain is associated with the singularity at $D \sim 2025$ and the exponent $M = 1$, which fairly correlates with von Forster et al. (1960) 'Hyperbolic, Doomsday' pattern, although they overestimated it for a 1500-year period, from 400 CE (von Foerster et al, 1960). The **inset in Figure 8** validates such scaling, but for a shorter period. After the crossover at ~1968, a 'tunelling' to a 'tail' of a reversed critical behavior hidden in the past

(~1919) occurs. Notably, the 'reversed' critical pattern causes the population to continue rising, but at a decreasing growth rate.

The main part of the plot shows that the critical-like scaling (Eq. (18)) offer also a fair description for 7 000 years of the Neolithic era., with singularity at $D = t_C \approx 1200BC$, related to $G_P^{-1}(t_C) = 0$. This is a surprising and precise correlation with the collapse and rapid integration of the great Bronze Age civilisations and empires in the Near East and Mediterranean regions. At the same time, the decline of the classical era of ancient Egyptian civilization began after the death of Pharaoh Ramesses II and his state-exhausting wars. The Bronze Era collapse is linked to climate change, geostorms, and, above all, the invasions of the so-called Sea Peoples (Glass, 2021). But perhaps the inhabitants of the Bronze Age empires (c. 3000–1000 BC) also felt enslaved by the increasing demands and burdens of imperial authorities, and took advantage of their weakening to retreat to the wider world beyond, where such oppressive power did not exist? Or perhaps they joined the Sea Peoples warriors? A similar explanation has been put forward two Millenia later, for the rapid decline of the Maya civilization on the Yucatán Peninsula in present-day Mexico and Guatemala (Turner & Sabloff, 2012). However, a surprising systemic determinism emerges, for inevitable change in the pattern for the global population

In this context, it is worth taking a critical look at the peculiarities revealed in **the inset of Figure 8**. As for $D_1 \approx 1919$, it is a fair coincidence with the end of World War I, which wiped out the great empires of Russia, Austria-Hungary, and Germany—dominant in Europe since the Congress of Vienna (1815)—from the map of Europe. The post-feudal order lost its significance. It was also during this period that the United States unequivocally demonstrated its global power (Lowe, 2015). When von Foerster et al.'s paper (1960) was published in 1960, it was not the usual Doomsday singularity, at $D_1 \approx 2026$. At the time, it seemed like an odd, random date without any particular significance. Now, however, we recognize that it has civilizational significance, as a New World Order is emerging, amid current world-impacted Wars.

6. Discussion: Avoided Criticality and the Carrying Capacity

The inset in **Figure 6**, shows that from 1800 till ~1966/8 the dominant trend can be approximated by a next empirical exponential equation (Drozd-Rzoska & Sojecka, 2026):

$$P(t) = P_0 \exp\left(\frac{t}{\tau}\right)^{\beta(t)}, \quad (20)$$

with the exponent changing from $\beta \sim 1$ to $\beta \sim 4$, which can be named as Hyper–Malthusian due to unique $\beta(t)$ changes.

The mentioned trend is 'disturbed in the post-WWII period', from ~1950 to ~ 1968, when the exponent $\beta \approx 1.5$ (Sojecka AA, Drozd-Rzoska, 2024). It can be associated with the post-WWII qualitative reset in the economy, social circumstances, and culture. The discussed period is associated with the increasingly compressed exponential relaxation (CER) dynamics. Such behavior, related to the exponent $\beta > 1$, has only recently been discovered in physical systems (Wu et al., 2018; Trachenko & Zaccone, 2021). It indicates the dominance of processes significantly 'faster' than the standard exponential case ($\beta = 1$, and Eq. (1)), also suggesting the presence of internal stresses that can lower energy barriers between different channels of processes developing in the given system, and facilitating rapid rearrangement - even in an avalanche-like manner.

From ~1968 till today, dynamics is dominated by the stretched exponential relaxation (SER) related to the exponent $\beta < 1$, as shown in the inset in **Figure 6**. SER-related dynamics can be associated with a large number of possible process channels, each with a low probability of being open. A shift between states can promote energy dissipation. This phenomenon is often observed in disordered physical systems, but the broad distribution of relaxation times associated with multichannel processes can also be linked to hierarchical constraints or to spatially heterogeneous systems that are locally ordered. The inset in **Figure 6** reveals a general crossover CER ($\beta > 1$) $\Rightarrow$ SER ($\beta < 1$), near the year 1968, for the global population ~3.5 billion.

Notably, such exceptional dynamics recall the Gardner transition pattern, which can generally be described as a crossover between two types of systems, 'mechanically' stable and 'marginally' stable. Near this transition, responses to endogenic and exogenic impacts are strongly nonlinear and are often associated with intermittent plastic events, while the system remains globally solid. Solidity breaks down at larger deformations, leading to 'complete' reorganization (Drozd-Rzoska & Sojecka, 2026; Berthier et al., 2019; Li et al., 2021). The authors argue that this fundamental pattern strongly correlates with permanent developments in the early Industrial Revolution and with the reorganization that followed WWII. For states /domains associated with SER ($\beta < 1$) dynamics, and local networking dominate, but when shifting away from a hypothetical singularity (the case of the global population), all of these weaken. Notably, the Gardner transition can be associated with avoiding criticality (Berthier et al., 2019; Li et al., 2021), the pattern evidenced above: Figure (8) and Eq. (20).

When discussing the results of this report, it is worth bearing in mind the issue of Carrying Capacity (Sojecka, Drozd-Rzoska & Rzoska, 2024). Notably, the enormous amount of reports on this topic, over the past decade, has made it central to discussions on sustainable development and ecology (del Monte-Luna, 2004; Wang, 2022; Bradshaw, 2026). While these papers provide quantitative estimates of this key parameter, the authors of the given find them significantly unsatisfactory, particularly with respect to fundamental justification. Such estimations require the selection of significant resources under consideration and their relationships, as well as multidimensional interpretative models, often biased by initial assumptions.

The authors of this paper prefer Cohen's concept (1995), which emphasizes the direct relationship between Carrying Capacity and population changes, to be more significant. In fact, it suggests focusing rather on the time trend for Carrying Capacity changes. Building on this, Cohen proposed the 'Condorcet' relation (Cohen, 1995):

$$\frac{\mathrm{d}K(t)}{\mathrm{d}t} = c(t)\frac{\mathrm{d}P(t)}{\mathrm{d}t} = \frac{L}{P(t)}\frac{\mathrm{d}P(t)}{\mathrm{d}t} \ , \qquad (21)$$

where $L = \text{const}$.

The authors of this report developed this dependence by introducing the analytic RGR factor (Sojecka , Drozd-Rzoska, Rzoska, 2025):

$$\Longrightarrow \quad \frac{\mathrm{d}K(t)}{\mathrm{d}t} = L \ \frac{1}{P(t)}\frac{\mathrm{d}P(t)}{\mathrm{d}t} = L\frac{\mathrm{d}\ln P(t)}{\mathrm{d}t} = LG_P \ . \qquad (22)$$

Following this, the RGR-related characterizations can provide insight into the evolution of Carrying Capacity. **Figures 7 & 8** are of particular interest, as they show the dominant trends in global population and Carrying Capacity across subsequent epochs, described by either the basic Malthusian dynamics (Equation (1)) or the critical growth trajectory (Equation (19)).

It should be noted that essentially the reference to the Verhulst–Pearl equation (3) describes population change using Malthus's model of infinite carrying capacity (C–C). Does this suggest a world of unlimited opportunities for a growing population in 'Malthus-relate' times ? Malthusian's dynamics is related to $G_P = \text{const}$. In such a situation, subsequent generations of a growing population can individually have the same share of the system's important resources (Carrying Capacity) as previous generations, as indicated by Eq. (22). This conclusion can be supported by carpenters' wages in England, which remained almost unchanged from the 13th century until the early 19th century. England can be considered a model country, as it has had unchanging borders, stable governments, and no 'invasions' by hostile neighbors over such a long period. For six centuries, the share of Carrying Capacity available to individuals remained almost unchanged. During the Industrial Revolution, which began in the 18th century, Carrying Capacity increased rapidly. According to Eq. (22) and **Figure 8**, the typical worker's share of this increase has remained unchanged since the Middle Ages.

Generally, during periods of 'critical' population growth, resources and Carrying Capacity, which are crucially related to creativity, work, innovative progress, and the development of social ties, ultimately lead to an increase in individual 'well-being', i.e., the proportion strong rise of personally available part in Carrying Capacity. **Figure 8** suggests that this situation occurred during the Neolithic era and the first 7,000 years of the Anthropocene. It was an era of increasing opportunity and possibility across generations. This was not repeated until the Industrial Revolution, until 1968.

Of course, after this year, the personal share of global success increases, but on a relative scale, it seems to decrease from generation to generation.

In this work and in the refs. (Sojecka, Drozd-Rzoska, Rzoska, 2025; Sojecka & Drozd-Rzoska, 2025; Sojecka & Drozd-Rzoska, 2024; Drozd-Rzoska & Sojecka, 2026), a new method of preparing population data using numerical filtering supported by Saviztky-Gilay protocol (Luo, et al., 2005) was implemented and demonstrated. This yielded an analytical dataset of 206 points describing population changes over more than 12,000 years. Importantly, this approach was based on an initial data collection from multiple sources, thereby avoiding potential bias that could arise from relying on a single source. Next, a distortion-sensitive test feedback analysis was used to combine empirical data and test model scaling relationships. We emphasize these issues because they fulfill the fundamental requirement of the scientific method: reliable, conclusive empirical validation.

The authors argue that the difficulty of achieving reliable empirical validation is a key factor in the long-term cognitive impasse surrounding the modelling of global population change. This is exemplified by the vast and utterly inconclusive range of predictions for the year 2100, as depicted in **Figure 2**. A second issue is the attempt to test model scaling relationships over long time periods — up to thousands of years and even the entire Anthropocene — without first demonstrating that such a description is fundamentally justified over these timescales. We emphasize this fact because the present work and the refs. (Sojecka, Drozd-Rzoska, Rzoska, 2025; Sojecka & Drozd-Rzoska, 2025; Sojecka & Drozd-Rzoska, 2024; Drozd-Rzoska & Sojecka, 2026) explicitly demonstrate that no single long-term scaling equation for global population changes in Anthropocene can exist.

The authors of the given report note that the aforementioned problems of empirical validation are endemic to many analyses reported to date. In this context, and with reference to the results presented in this work, the authors would like to address two very recent trend-setting works (Zaccone & Trachenko, 2026; Yakovenko, 2026).

Representative can be two recent works which, in addition to offering interesting conceptual results, also demonstrate the aforementioned problem (Zaccone &Trachenko, 2026):

$$\frac{\mathrm{d}P(t)}{\mathrm{d}t} = b \times P(t) - dP(t) = (b-d)P(t) = r(t)P(t) = \frac{\exp[KP(t)]}{\tau}P(t), \tag{23}$$

where b and d are the birth rate per element per unit time and the death rate per element per unit time, respectively, and $r = b - d$ is known as the 'productivity of the individual element'. Further, it was assumed that $r(t) = \exp\big(KP(t)\big)/\tau$, $\tau = \mathrm{const}$, and $K = \mathrm{const}$.

The above means that τ is here an empirical constant, not the relaxation time discussed above. The authors of ref. (Zaccone & Trachenko) consider the above for the coefficient $K > 0$ as reflecting the stretched exponential function (SEF) dynamics and $K < 0$ as the compressed exponential. Further, recalling the empirical evidence, the discussion of the Zaccone-Trachenko relation (2026), proposed to describe relaxation in glass-forming materials following perturbative stress (mechanical, electrical, …), was adopted due to its formal similarity to Eq. (23). It led the author of ref. (Zaccone A, Trachenko, 2026). Later, it was noted that for $K < 0$ and developing the exponent in Eq. (23) in a Taylor series, the Verhulst equation is recovered. For $K > 0$ the authors indicated that Eq. (23) has the Ricatti differential equation form (Zaccone A, Trachenko, 2026): one of the solutions is von Foerster et al. (1960) type 'hyperbolic' equation, although conditions of such solutions in the frames of the population characterizations are not satisfactorily explained. Finally, to take into account the Carrying Capacity, the 'universal' carrying capacity impact was taken into account (Zaccone A, Trachenko, 2026):

$$\frac{\mathrm{d}P(t)}{\mathrm{d}t} = \frac{\exp[KP(t)]}{\tau}P(t)\left[1 + \frac{P(t)}{\kappa}\right], \tag{24}$$

where κ is the Carrying Capacity.

The problem constitues the multiparameter nature of the final relation describing changes in $P(t)$, which also uses an arbitrarily chosen reference constant value for Carrying Capacity, κ, ultimately leading to the prediction of a maximum population in 2064 (Zaccone A, Trachenko, 2026).

It should be recalled that $1/\kappa$ means the maximum sustainable population size given the population's essential resources. Therefore, the assumed value of Carrying Capacity κ

essentially defines when the stationary phase or population maximum occurs in the Verhulst-type equation, to which the relation introduced in ref. (Zaccone A, Trachenko, 2026) can be encountered. Then, assuming the value of κ, one assumes the eventual appearance and value of the global population a priori.
Despite the suggestion of the universality of the description from the beginning of the Anthropocene to the present, no explicit validation against 'empirical' data has been carried out in ref. (Yakovenko, 2026).

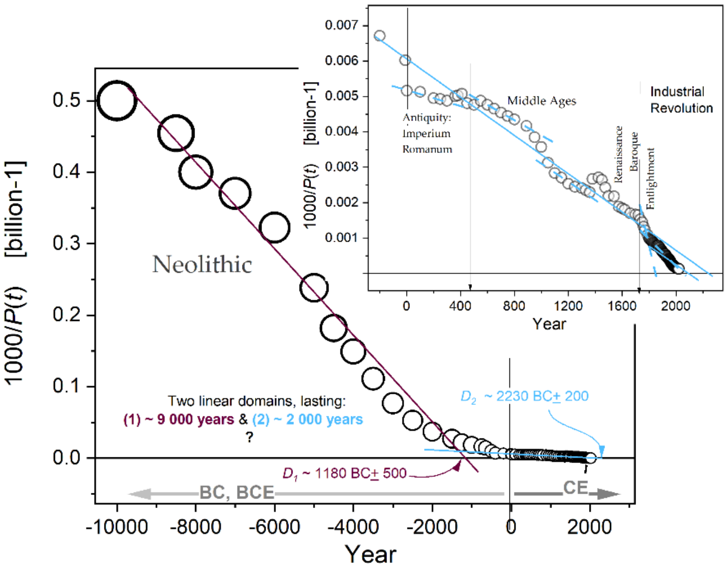

Figure 9. The normalized reciprocal of global population in Anthropocene focused on the direct apparent validation of von Forster et al. (1960). Hyperbolic scaling, i.e., via Eq. (7) with the exponent $M = 1$, indicated by linear patterns. The inset shows the focused behavior for the last two millennia. The dashed lines indicate a set of 'apparent linear domains' matched with von Foerster et al. scaling.

The next issue that should be treated with caution is the reference scale used to analyze the results. The importance of this factor was already indicated in the discussion of 'Doomsday' scaling by von Foerster et al. (1960). Another option for analysis to justify preferences is the 'reciprocal scale' analysis:

$$P(t) = \frac{A}{D-t} \qquad \Rightarrow \qquad \frac{1}{P(a)} = (A^{-1}D) - A^{-1}t. \tag{25}$$

Validations based on the representation of changes on the scale of $1/P(t)$ vs. t were used, for example, in (Yakovenko, 2026).
The authors of the given report present such an analysis in **Figure 9**. The central part of the plot reveals two domains described by the above relation. The first period, spanning more than 8,000 years from 10,000 BC to around 1500 BC, aligns remarkably well with the findings of the distortion-sensitive analysis depicted in Figure 8. This includes a 'critical anomaly around 1180 BC', which coincides precisely with the collapse of Bronze Age civilizations. Another 'hyperbolic' anomaly appears from antiquity to the present, with an apparent singularity at ~2230. However, as the **insight in Figure 9** shows, such an anomaly does not exist. This is the result of 'scale compression' in analyses based on Eq. (25). Such 'compression' is particularly strong in cases involving gigantic, multi-decadal changes in values — the feature exhibited by global population changes.

8. Conclusions:

This report presents a new approach to modelling global population dynamics, implementing the category of Active Soft Matter as the fundamental reference. More specifically, it implements the subcategory proposed by the authors (Drozd-Rzoska & Sojecka): Human Active Intelligent Soft Matter. Global population changes were then tested using universal model equations applicable to complex Soft Matter systems. Of particular significance are the super-Malthusian equation and critical-like scaling (Sojecka & Drozd-Rzoska, 2024). The Soft Matter provides a well-justified, fundamental basis for interpreting the parameters in fitted scaling equations, thereby shedding new light on global population dynamics. It offers qualitative supplementation to the standard demographic approaches (see the **1st** and **2nd** cognitive **Paths** above). It is worth noting that the different Soft Matter based scaling relations enable us to identify and highlight the distinct process features that govern global population changes.

The introduction of distortion-sensitive analysis using the Analytic Relative Growth Rate (Sojecka & Drozd-Rzoska, 2025), is particularly important for the ultimate validation of the model descriptions discussed.

The analysis presented in this paper clearly demonstrates the non-monotonic nature of global population change in the Anthropocene. This makes it fundamentally inappropriate to describe global population changes using a single model equation in arbitrarily selected longer periods. First, it is necessary to verify the adequacy of a given description within a selected time period or epoch, as demonstrated by the methodology presented in this report. A notable outcome of this study is the strong correlation between changes in global population characteristics and specific historical events, reflecting the internal dynamics of extremely complex Human Active Intelligent Soft Matter. This also allows us to identify those events that may have had a global impact.

In conclusion, in light of the 'forecasts till 2100 challenge', this report does not identify validated hallmarks of a future decline in the global population. Instead, the growth, albeit at a slower rate, can be expected. Extrapolating the prevailing trend of recent decades suggests that the global population could reach 14 billion by 2100.

Conflicts of Interest: The authors declare no conflict of interest.

References

1. Amaral MA, de Oliveira AM. Criticality and Griffiths phase in random games with quenched disorder. Phys Rev E, 2021; 104: 064102. DOI: 10.1103/PhysRevE.104.064102
2. Bacaër N. "Histoires de Mathématiques et de Populations." Paris: Cassini; 2008.
3. Baulin VA, et al. Intelligent Soft Matter: towards embodied intelligence. Soft Matter 2025, 21, 4129-4145.
4. Berthier L, Biroli G, Charbonneau P, Corwin EI, Franz S, Zamponi F. Gardner physics in amorphous solids and beyond. J Chem Phys 2019; 151: 010901. DOI: 10.1063/1.5097175
5. Bradshaw CJA et al. Global human population has surpassed Earth's sustainable carrying capacity Environ. Res Lett. 2026; 21: 064023. DOI: 10.1088/1748-9326/ae51aa
6. Bystroff C. Footprints to singularity: A global population model explains late 20th century slow-down and predicts peak within ten years. PLoS One. 2021; 16: e0247214. DOI: 10.1371/journal.pone.0247214
7. Cameron IR. "Nuclear Fission reactors." Berlin: Springer; 2011.
8. Cavagna A, Del Castello L, Dey S. et al. Short-range interactions versus long-range correlations in bird flocks. Phys Rev E. 2015; 92: 012705. DOI: 10.1103/PhysRevE.92.012705
9. Cecconi F, Cencini M, Falcioni M, Vulpiani A. Predicting the future from the past: An old problem from a modern perspective. Am J Phys. 2012; 80:1001–8. DOI: 10.1119/1.4746070
10. Chrapeć J, Rzoska SJ, Zioło J. Pseudospinodal curve for binary solutions determined from the nonlinear dielectric effect. Chem Phys. 1987; 111: 155-160. DOI: 10.1016/0301-0104(87)87017-9
11. Cohen JE. Population growth and Earth's human carrying capacity. Science. 1995; 269: 341–346. DOI: 10.1126/science.7618100
12. Dai J, Chen S. The application of ARIMA model in forecasting population data. J Phys: Conf Ser. 2019; 1324: 012100. DOI: 10.1088/1742-6596/1324/1/012100
13. Das M, Schmidt, CF, Murrel M. Introduction to Active Matter. Soft Matter. 2020; 16: 7185-7190. DOI: 10.1016/j.physrep.2014.10.001
14. Douglas B. "Plagues and Pandemics: Black Death, Coronaviruses and Other Killer Diseases Throughout History." London: Barnsley; 2022.
15. de Gennes PG, Badoz J. "Fragile Objects: Soft Matter, Hard Science, and the Thrill of Discovery. Göttingen, Germany: Copernicus; 1996. DOI: 10.1017/S0883769400029171
16. Dolgonosov M, Naidenov VI. An informational framework for human population dynamics. Ecol Mod. 2006; 198: 375-386. DOI: 10.1016/j.ecolmodel.2006.05.004
17. Deevey ES. Of Doomsday and the lower Mississippi. Science. 1987; 238: 1215. DOI: 10.1126/science 3685968_
18. del Monte-Luna P, Brook BW, Zettina-Rejon MJ, Cruz-Escalona VH. The carrying capacity of ecosystems. Global Ecology and Biogeography. 2004; 13: 485-495. DOI: 10.1111/j.1466-822X.2004.00131.xDigital Object Identifier (DOI)

19. Dias A, D'Hombres M, Ghisetti B, Pontarollo C, Dijkstra N. The determinants of population growth: literature review and empirical analysis. Working Papers -10, Joint Research Centre, European Commission. 2018. DOI: 10.2760/513062
20. Dochy F. Human population growth: local dynamics - global effects. Acta Bioltheoretica. 1995; 43: 241-247. DOI: 10.1007/BF00707272)
21. Drozd-Rzoska A, Rzoska SJ, Starzonek S. New scaling paradigm for dynamics in glass-forming systems. Prog Mat Sci 2023; 134:101074. DOI: 10.1016/j.pmatsci.2023.101074
22. Drozd-Rzoska A. 2019 Universal behavior of the apparent fragility in ultraslow glass forming systems. Sci. Rep. 9, 6816. DOI: 10.1038/s41598-019-42927-y
23. Drozd-Rzoska A. Sojecka AA. Critical and Soft Matter view on global population dynamics. Royal Soc. Open Sc. ID is RSOS-260946
24. Ehlers J, Gibbard P.L. The extent and chronology of Cenozoic Global Glaciation. Quaternary International 2007: 164–165, 6–20. DOI: 10.1016/j.quaint.2006.10.008
25. Everitt A. "Cicero: The Life and Times of Rome's Greatest Politician." New York: Random House; 2003.
26. Espinosa RME, Koh SC. Forecasting the ecological footprint of G20 countries in the next 30 years. Sci Rep 2024; 14: 8298. DOI: 10.1038/s41598-024-57994-z
27. Flies EJ, Brook BW, Blomqvist L, Buettel JC. Forecasting future global food demand: A systematic review and meta-analysis of model complexity. Environment Int. 2018; 120: 93-103. DOI: 10.1016/j.envint.2018.07.019
28. Fraser-Smith AC. Space science strategy. Eos Trans Am Geophys Union. 1989; 70: 1569. DOI: 10.1029/89EO00399)
29. Garnsey P. "The Roman Empire: Economy, Society and Culture." Oakland: University of California Press; 2014.
30. Gierliński GD. Niedźwiedzki G, Lockley MG, et al. Possible hominin footprints from the late Miocene (c. 5.7 Ma) of Crete? Proc Geolog Assoc. 2017, 128; 2017: 697-710. DOI: 10.1016/j.pgeola.2017.07.006.
31. Glass B. "The Anthropocene Epoch. When Humans Changed the World."Houston: DBG Publishing; 2021. ISBN: 978-0578995304.
32. Gonzalo JA, Alfonseca MFF. "World Population: Past, Present, & Future." Singapore: World Scientific; 2016. ISBN: 978-9813140998
33. Grine FE, Fleagle JG. The First Humans: A summary perspective on the origin and early evolution of the Genus Homo. In: Grine FE, Fleagle JG, Leakey RE. (eds) "The First Humans – Origin and Early Evolution of the Genus Homo. Vertebrate Paleobiology and Paleoanthropology." Dordrecht: Springer; 2009. DOI: 10.1007/978-1-4020-9980-9_17
34. Gonzalez-Rodriguez D, Guevorkian K, Douezan S, Brochard-Wyart F. Soft matter models of developing tissues and tumors. Science. 2012; 338: 910-927. DOI: 10.1126/science.1226418
35. Gu D, Andreev K, Dupre ME. Major trends in population growth around the world. China CDC Weekly. 2021; 9: 604–613. DOI: 10.46234/ccdcw2021.160
36. Harper WL. "Isaac Newton's Scientific Method: Turning Data into Evidence About Gravity and Cosmology. "Oxford: Oxford University Press; 2012.
37. Huang C, Ling F, Kanso E. 2024 Collective phase transitions in confined fish schools, Proc. Natl. Acad. Sci. USA 121, e2406293121. DOI: 10.1073/pnas.2406293121
38. Hu D, Phonekeo S, Altshuler E. et al. Entangled active matter: From cells to ants. Eur Phys J Spec Top 2016; 225: 629–649. DOI: 10.1140/epjst/e2015-50264-4
39. Hutton WE. Doomsday. Science. 1961; 133: 937-939. DOI: 10.1126/science.133.3456.937
40. Howland WW. Doomsday. Science. 1961; 133: 939-940. DOI: 10.1126/science.133.3456.939
41. Herrington G. Update to limits to growth: Comparing the World3 model with empirical data. J Ind Ecol. 2020; 25(3): 614–26. DOI: 10.1111/jiec.13084
42. Hill RC, Griffiths WE, Lim GC. "Principles of Econometrics." New York: John Wiley & Sons; NY: 2011.
43. Holman G. "The Scientific Method: Why Science is a Crucial Process for Human Progress, not Just Another Academic Subject or Belief." London: Independently published; 2023.
44. Hough RR. Doomsday, the Internet, diversity, and sustainability. Systems Research. 1996; 13: 287-292. DOI: 10.1002/(SICI)1099-1735(199609)13:3<287
45. Hu W, Hao Z, Du, PD F. di Vincenzo G, et al. Genomic inference of a severe human bottleneck during the Early to Middle Pleistocene transition. Science. 2023:381; 979-984. DOI: 10.1126/science.abq7487
46. Iannelli M, Pugliese A. "An Introduction to Mathematical Population Dynamics: Along the Trail of Volterra and Lotka." Berlin: Springer; 2014.
47. Janzen G, Maselli G, Jimenez JF, Garcia-Perez L, Matoz Fernandez DA. Active Matter as a framework for living system inspired. Robophysics 2026; https://arxiv.org/html/2511.14624v2
48. Jones RAL. "Soft Condensed Matter." Oxford: Oxford Univ. Press.; 2002.
49. Kac S, Lutz W. The human core of the shared socioeconomic pathways: Population scenarios by age, sex and level of education for all countries to 2100. Glob Environ Change. 2017; 42: 181–92. DOI:10.1016/j.gloenvcha.2014.06.004 PMID: 28239237

50. Keilman N. Uncertainty in population forecasts for the twenty-first century. Ann Rev Res Econ. 2020; 12: 449-470. DOI: 10.1146/annurev-resource-110319-114841
51. Kapitza SP. On the theory of global population growth. Phys.-Uspekhi 2010; 53: 1287–96. DOI: 10.3367/ufne.0180.201012g.1337
52. Katul GG. Fifty years to prove Malthus right. Proc Natl Acad Sci USA. 2013; 110: 4161–4162. DOI: 10.1073/pnas.1301246110
53. Kendall BE, Fox GA, Fujiwara M, Nogeire TM. Demographic heterogeneity, cohort selection, and population growth. Ecology. 2011;9 2:1985–93. DOI: 10.1890/11-0079.1 PMID: 22073789
54. Kremer A. Population growth and technological change: one million B.C. to 1990. The Quarterly J Economy. 1993; 108: 681-716. DOI: 10.2307/2118405
55. Lam D. The next 2 billion: can the world support 10 billion people. Population and Development Review. 2024; 51; 63-102, . DOI: 10.1111/padr.12685
56. Lai CD, Murthy D, Xie M. 2006 Weibull Distributions and their applications. In: Pham, H. (eds) "Springer Handbook of Engineering Statistics." London: UK; Springer.
57. Lima M, Berryman AA. Positive and negative feedbacks in human population dynamics: future equilibrium or collapse?. Oikos. 2011; 120: 1301–1310. DOI: 10.1111/j.1600-0706.2010.19112.x
58. Lehman C, Loberg S, Wilson M, Gorham E. Ecology of the Anthropocene signals hope for consciously managing the planetary ecosystem. Proc Natl Acad Sci USA. 2021; 118(28): e2024150118. DOI: 10.1073/pnas.2024150118
59. Li H, Jin Y, Jiang Y, Jeff Z, Chen Y. Determining the nonequilibrium criticality of a Gardner transition via a hybrid study of molecular simulations and machine learning. Proc Natl Acad Sci USA. 2021; 118: e2017392118. DOI: 10.1073/pnas.201739211
60. Lima M. The link between human population dynamics and energy consumption during the Anthropocene. The Anthropocene Review 2024; 12: 1-25. DOI: 10.1177/20530196241255081
61. Lima M, Berryman AA. Positive and negative feedbacks in human population dynamics: future equilibrium or collapse?. Oikos. 2011;120(9):1301–10. DOI: 1111/j.1600-0706.2010.19112.x
62. Lowe N. Mastering Modern World History. London: Pilgrave; 2015.
63. Luo J, Ying K, Bai J. 2005 Savitzky–Golay smoothing and differentiation filter for even number data. Signal Processing 85, 1429-1434. DOI: 10.1016/j.sigpro.2005.02.002.by
64. Mallamace F, Branca C, Corsaro C, Leone N, Spooren, J, Chen S-H, Stanley HE. Transport properties of glass-forming liquids suggest that dynamic crossover temperature is as important as the glass transition temperature. Proc Natl Acad Sci USA. 2010; 107: 22457-22462. DOI: 10.1073/pnas.1015340107
65. Malthus T. An Essay on the Principle of Population. London: John Murray; 1798. ISBN: 978-1680922585.
66. McFarlane I. State world population report 2023. 8 billion lives, infinite possibilities – the case for rights and choices. UNFPA; New York: 2023. www.unfpa.org/swp2023.
67. MacIntyre F. The Maltho-Marxian hypothesis 'economics controls population': a test and a projection. Population Review. 2005; 44: 24-49. DOI: 10.1353/prv.2006.0003
68. Martinez-Garcia JC, Rzoska SJ, Drozd-Rzoska A, Martinez-Garcia J. A universal description of ultraslow glass dynamics. Nature Comm. 2013; 4: 1823. DOI: 10.1038/ncomms2797
69. Menzel AM. Tuned, driven, and active Soft Matter. Phys Rep. 2015; 554: 1-45. DOI: 10.1016/j.physrep.2014.10.001
70. Narayan U, Saikia P, Mahanta DJ. 2022 A review of the growth models in biological sciences. AIP Conf Proc. 2451, 020070. DOI: 10.1063/5.0095187
71. Pearl R, Reed LJ. On the rate of growth of the population of the United States since 1790 and its mathematical representation. Proc Natl Acad Sci USA. 1920; 6: 275–288. DOI: 10.1073/pnas.6.6.275
72. Pearl R. The growth of populations. Quaternary Review in Biology. 1927; 2: 532–548. DOI: 10.1126/science.66.1702.x.t
73. Podum E, Whither FEH.the life-support system?, pp.263-290. In: N. Polunin, (editor) "Growth without Ecodisasters?". London: Palgrave Macmillan; 1980. DOI: 10.1007/978-1-349-03680-6_9
74. Raftery AE, Ševčíková H. Probabilistic population forecasting: Short to very long-term. Int J Forecast. 2023; 39: 73–97. DOI:10.1016/j.ijforecast.2021.09.001
75. Ribeiro FL. An attempt to unify some population growth models from first principles. Rev Bras Ensino Fís. 2017: 39; 1. DOI: 10.1590/1806-9126-RBEF-2016-0118
76. Robertson JS, Bond VP, Cronkite EP. 1961 Doomsday. Science. 1961; 133: 936-937. DOI: 10.1126/science.133.3456.936
77. Rzoska SJ, Degiorgio V, Bellini T, Piazza R. Relaxation of the electric birefringence near a critical consolute point. Phys. Rev. E. 1994; 49: 3093-3096. DOI: 10.1103/PhysRevE.49.3093
78. Rzoska SJ, Zioło J, Drozd-Rzoska A. Stretched-relaxation after switching-off a strong electric field in a critical solution under high pressure. Phys Rev E. 1997; 56: 2578-2581. DOI: 10.1103/PhysRevE.56.2578
79. Rzoska SJ, Mazur V. 2007 Soft Matter under Exogenic Impacts. Berlin, Germany: Springer. DOI: 10.1007/978-1-4020-5872-1

80. Rzoska SJ, Drozd-Rzoska A. Dual field nonlinear dielectric spectroscopy in a glass forming EPON 828 epoxy resin. Phys: Condens Matter, 2011; 24: 035101. DOI: 10.1088/0953-8984/24/3/035101
81. Saridakis EN. Do we need Soft Cosmology. Phys Lett B. 2021; 822: 136649. DOI: 10.1016/j.physletb.2021.136649
82. Sawada T. Filamentous virus-based soft materials based on controlled assembly through liquid crystalline formation. Polym J. 2017; 49: 639–647. DOI: 10.1038/pj.2017.35
83. Semerano M, Negro G, Marenduzzo D, Forte G. Modelling transcriptional silencing and its coupling to 3D genome organisation. Soft Matter. 2025; 21: 6975–6983. DOI: 10.1039/d5sm00686d
84. Serra F, Tkalec U, Lopez-Leon T. Topological Soft Matter. Front Phys. 2020; (Special Issue).
85. Serrina J. Is Doomsday on Target? Science. 1975; 189: 86-88. DOI: 10.1126/science.189.419
86. Shinbrot M. Doomsday. Science 33, 1961, 940-943. DOI 10.1126/science.133.3456.940
87. Shumway RH, Stoffer DS. "Time Series Analysis and Its Applications." Berlin: Springer; 2017. DOI: 10.1007/978-3-319-52452-8
88. Siegel FR. "Population Assessments: 2013–2050–2100: Growth, Stability, Contraction." In: Springer Briefs in Environmental Science. Berlin: Springer; 2015. DOI: 10.1007/978-3-319-09686-5_1
89. Smith DA. Human population growth: stability or explosion. Mathematics Magazine. 1977; 50: 186-197. DOI: 10.1080/0025570X/1977.11976645
90. Stanley HE. Introduction to Phase Transitions Critical Phenomena. Oxford: Oxford Univ. Press, 1989.
91. Sojecka AA, Drozd-Rzoska A. The story about one island and four cities: the socio-economic soft matter model – based report. Proc Socrat Lect. 2023; 8: 131. DOI: 10.55295/PSL.2023.II18
92. Sojecka AA, Drozd-Rzoska A, Rzoska SJ. Food preservation in the Industrial Revolution Epoch: Innovative High Pressure Processing (HPP, HPT) for the 21st-Century Sustainable Society. Foods 2024; 13: 3028. DOI: 10.3390/foods13193028
93. Sojecka AA, Drozd-Rzoska A. Global population: from Super-Malthus behaviour to Doomsday criticality. Scientific Reports. 2024; 14: 9853. DOI: 10.1038/s41598-024-60589-3
94. Sojecka AA, Drozd-Rzoska A. Society & Science: Criticality for the global society. Proc Socrat Lect. 2025; 12(II): 155. DOI: 10.55295/PSL.12.2025.II16
95. Sojecka AA, Drozd-Rzoska A, Rzoska SJ. Global population growth, carrying capacity, and high-quality foods in the Industrial Revolutions epoch. Sustainability. 2025; 17: 6827. DOI: 10.3390/su17156827
96. Sojecka AA, Drozd-Rzoska A. Verhulst-type equation and the universal pattern for global population growth. PLoS ONE. 2025; 20: e0323165. DOI: 10.1371/journal.pone.0323165
97. Shpurov I, Froese T. Evidence of critical dynamics in movements of bees inside a hive. Entropy. 2022; 24: 1840, DOI: 10.3390/e24121840
98. Stokstad E. Will Malthus continue to be wrong?. Science. 2005; 309: 102. DOI: 10.1126/science.309.5731.102
99. Stutz LN, Peyroteo Stjerna R, Tõrv M. "The Oxford Handbook of Mesolithic Europe." Oxford: Oxford Academic, 2025. DOI: 10.1093/oxfordhb/9780198853657.013.9, accessed 16 May 2026
100. Taagepera R. People, skills, and resources: an interaction model for world population growth. Technol. Forecast Soc Changes. 1979; 13: 13-30. DOI: 10.1016/0040-1625(79)90003-9
101. Taagapera R, Nemčok, M. World population growth over millennia: Ancient and present phases with a temporary halt in-between. The Anthropocene Review. 2023; 11: 163-168. DOI: 10.1177/205301962311724
102. Taagapera R, Nemčok M. "More People. Fewer States. The past and future of World Population and Empire States." Cambridge: Cambridge Univ. Press.; 2024.
103. Tang XJ. Opportunities and challenges in biological soft matter research. Opportunities and challenges in biological soft matter research. Front Soft Matter. 2022; 2: 958524. DOI: 10.3389/frsfm.2022.958524
104. Thedford RP, et al. The promise of Soft Matter enabled quantum materials. Advanced Materials 2023; 5: 220398. DOI: 10.1002/adma.202203908
105. Trachenko K, Zaccone A. Slow stretched-exponential and fast compressed-exponential relaxation from local event dynamics. J. Phys: Condens Matter 2021; 33: 315101. DOI: 10.1088/1361-648X/ac04cd
106. Turner BL, Sabloff JA. Classic Period collapse of the Central Maya Lowlands: Insights about human–environment relationships for sustainability. Proc Natl Acad Sci USA. 2012; 109: 13908–13914. DOI: 10.1073/pnas.1210106109
107. Umpleby SA. What I learned from Heinz von Foerster about the construction of science. Kybernetes. 2005; 34: 278–294. DOI: 10.1108/03684920510575843)
108. UNESA: United Nations, Dept. Econom. & Social Affairs, Population Division, World Population Prospects 2024; available at: https://population.un.org/wpp/; access 1 April 2026.
109. UNFPA: United Nations Population Fund (2026): https://www.unfpa.org/data/world-population-dashboard
110. van Witteloostuijn A, Vanderstraeten J, Slabbinck H, Dejardin M, Hermans J, Coreynen W. From explanation of the past to prediction of the future: A comparative and predictive research design in the Social Sciences. Social Sciences & Humanities Open. 2022; 6: 100269. DOI: 10.1016/j.ssaho.2022.100269

111. Varfolomeyev SD, Gurevich KG. The hyperexponential growth of the human population on a macrohistorical scale. J Theor Biol. 2001; 212: 367-372. DOI: 10.1006/jtbi.2001.2384
112. Verhulst PF. Deuxieme Memoire sur la Loi d'Accroissement de la Population. Mémoires de l'Académie Royale des Sciences, des Lettres et des Beaux-Arts de Belgique in EuDML. 1847; 20: 1–32. https://eudml.org/doc/178976
113. Vollset SE, Goren E, Yuan C-W, Cao J, Smith AE, Hsiao T, et al. Fertility, mortality, migration, and population scenarios for 195 countries and territories from 2017 to 2100: a forecasting analysis for the Global Burden of Disease Study. Lancet. 2020; 396(10258): 1285–306. DOI: 10.1016/S0140-6736(20)30677-2
114. von Foerster H, Mora PM, Amiot LW. Doomsday: Friday 13 November, A.D. 2026. Science. 1960; 32: 1291-1295. DOI: 10.1126/science.32.3436.1291
115. von Hoerner S. Population explosion and interstellar expansion. J British Interplanetary Soc. 1975; 28: 691-712. bib code 1975JBIS...28..691V
116. Umpleby SA. World population: still ahead of schedule. Science. 1987; 237: 1555-1556. DOI: 10.1126/science.237.4822.1555.c
117. Wang X. Managing land carrying capacity: key to achieving sustainable production systems for food security. Land .2022; 11: 484; DOI: 10.3390/land11040484
118. Wickham C. Medieval Europe. Yale University Press; New Haven: 2016..
119. WPR: World Population Review, March 10, 2026, Available from:: https://worldpopulationreview.com/
120. Wrugt Te. "Artificial Intelligence and Intelligent Matter. Nanoscience. Soft Matter. Philosophy." Berlin; Springer: 2026.
121. Wu ZW, Kob W, Wang WH, et al. Stretched and compressed exponentials in the relaxation dynamics of a metallic glass-forming melt. Nat Commun. 2018; 9: 5334. DOI: 10.1038/s41467-018-07759-w
122. Zaccone A, Trachenko K. Global population crisis scenarios predicted by the most general dynamic model/Available at https://arxiv.org/abs/2502.19063; accessed: 1st March, 2026.
123. Zhang W. A forecast analysis on world population and urbanization process. Environ Dev Sustain. 2008; 10: 717–730. DOI: 10.1007/s10668-007-9081-8
124. Yakovenko VM. The end of hyperbolic growth in human population and CO_2 emissions, Physica A. 2026; 661:130412. DOI: 10.1016/j.physa.2025.130412
125. Yumei Yu, Wendi Wang, Zhengyi Lu, Global stability of Gompertz model of three competing populations, J Math Anal Appl. 2007; 334: 333-348. DOI: 10.1016/j.jmaa.2006.12.060.